Simple benchmark for evaluating self-shielding models

ANS MC2015 - Joint International Conference on Mathematics and Computation (M&C), Supercomputing in Nuclear Applications (SNA) and the Monte Carlo (MC) Method · Nashville, Tennessee · April 19–23, 2015, on CD-ROM, American Nuclear Society, LaGrange Park, IL (2015)

SIMPLE BENCHMARK FOR EVALUATING SELF-SHIELDING MODELS

Nathan A. Gibson, Kord Smith, and Benoit Forget
Massachusetts Institute of Technology
77 Massachusetts Ave, Rm 24-214, Cambridge, MA 02141
ngibson@mit.edu; kord@mit.edu; bforget@mit.edu

ABSTRACT

Accounting for self-shielding effects is paramount to accurate generation of multigroup cross sections for use in deterministic reactor physics neutronics calculations. Historically, equivalence in dilution and subgroup techniques have been the preeminent means of accounting for these effects, but recent work has proposed new solutions, including the Embedded Self-Shielding Method (ESSM). This paper presents a very simple benchmark problem to compare these and future self-shielding methods.

The benchmark is perhaps the simplest problem in which both energy and spatial self-shielding effects are important, a two-region problem with a lumped resonant material. A single resonance in a single energy group is considered. Scattering is approximated using the narrow resonance approximation, decoupling each energy value and allowing an easily-computed reference solution to be obtained.

Equivalence in dilution using two-term rational expansions and the subgroup method were both found to give very accurate solutions on this benchmark, with errors less than 1% in nearly all cases. One-term rational expansions and ESSM showed much larger errors.

Key Words: self-shielding, benchmark, multigroup, cross sections

1 INTRODUCTION

The generation of accurate multigroup cross sections is central to the success of deterministic reactor physics neutronics calculations. Because of the complexity of nuclear cross section data, which contains large resonances, this process is difficult to perform accurately. The neutron flux exhibits depressions in energy near the resonances, an effect that has both spatial and energy implications known as self-shielding. This self-shielding effect is typically accounted for using an approximate model, such as equivalence in dilution [1, 2] or the subgroup method [3–5]. Recent work has sought to improve the self-shielding approximations and has resulted in new techniques such as the Embedded Self-Shielding Method [6].

The benchmark presented in this paper was originally intended to be an educational exercise, to give students an appreciation of the quality of the approximations typically encountered in a reactor physics calculation. However, the results warranted interest beyond a simple educational tool. Although equivalence in dilution methods have been studied extensively on very simple problems [7], side-by-side comparisons of these methods with the subgroup method on problems

where both are expected to perform well are not readily found. Furthermore, with the advent of newer self-shielding techniques, it is common to only see performance analysis on large problems. Ignoring very simple problems can lead to overlooking fundamental aspects of a technique and risks relying on cancellation of error for accuracy on specific problems.

Thus, this paper presents the simplest problem in which both energy and spatial effects are important in a self-shielding problem. It is designed such that the assumptions in self-shielding methods are fully valid, allowing the performance of a method to be understood without complications from poor assumptions. Results are presented for various self-shielding methods with some commentary about the effectiveness and the ease of use of each method.

2 BENCHMARK DESCRIPTION AND SPECIFICATIONS

2.1 Overview

The benchmark is representative of light water reactor conditions. Geometrically, equivalence-based self-shielding models assume two regions—fuel and moderator. Thus, this benchmark contains exactly those regions. Because self-shielding models typically only treat one resonant isotope at a time, this benchmark contains only one such isotope. This benchmark uses the most common assumption for the scatter source in self-shielding models, the narrow resonance approximation, and only a single energy group is considered.

Two classes of geometries are considered, an isolated slab and an infinite array of identical pin-cells, referred to as a "reflected pin-cell." Various widths of the slab and radii of the pin are considered to test a wide variety of shielding states. Two classes of resonances are considered, a square resonance and a single-level Breit-Wigner resonance. For the purpose of clarity in the results, only a single resonance is included in the resonant material.

The fuel material is assumed to have a constant cross section background moderator representative of U-238 in a light water reactor fuel pin. The resonant isotope is given a potential scattering cross section equivalent to that of U-238. The moderator material is assumed to be purely scattering. Its properties are chosen to be representative of water in a pressurized water reactor.

The quantity of interest is the group-averaged capture cross section of the resonant isotope. This is the output from a typical self-shielding calculation. The capture cross section is used rather than the total cross section, as it considers only the aspect of the cross section affected by self-shielding, whereas the total cross section would in large part be influenced by the constant potential scattering cross section.

This benchmark can be easily extended to cases not considered here. Some simple examples include varying the pin pitch, adding additional resonances to the fuel material, and changing the background level. Larger changes, breaking the assumptions in some self-shielding methods, include introducing cladding to the geometry, including a second resonant isotope, and using a more realistic scattering model.

2.2 Specifications

2.2.1 Geometry

Isolated Slab For the case of the isolated slab, the benchmark geometry is a one-dimensional configuration with a slab of lumped resonant material surrounded by an infinite medium of moderating material. In this case, the only parameter needed to define the configuration is the width of the slab. A slab width of $0.4\,\mathrm{cm}$ is the most analogous case to a pin found in a light water reactor. However, this parameter is varied to evaluate the accuracy of self-shielding methods over a range of configurations. The results presented in this paper include widths of $0.3\,\mathrm{cm}$, $0.4\,\mathrm{cm}$, and $0.6\,\mathrm{cm}$, but these can be varied over a larger range for methods verification.

The fuel slab should be treated as a single region for the purpose of determining the effective cross section. That is, this benchmark does not attempt to determine the spatial distribution of group cross section within the slab, but rather focuses only on the prediction of the spatial- and energy-averaged cross section. This is to maintain the assumption of a two-region problem.

Reflected Pin-Cell For the case of the reflected pin-cell, the benchmark geometry is a two-dimensional configuration with a cylindrical lump of resonant material surrounded by moderator in an infinitely repeating lattice. The only parameter varied in this benchmark is the fuel radius. The most realistic value for a pressurized water reactor is $0.4\,\mathrm{cm}$, and results are presented for radii of $0.3\,\mathrm{cm}$, $0.4\,\mathrm{cm}$, and $0.6\,\mathrm{cm}$. These can be varied over a larger range for methods verification. The pitch is held constant at $1.26\,\mathrm{cm}$ in this paper but can be varied in subsequent studies.

As with the slab, the pin and the moderator regions should be treated as single regions for the determination of effective cross sections in order to maintain the two-region assumption.

2.2.2 Physics

Energy Group A single energy group is used with group boundaries $1000\,\mathrm{eV}$ and $1100\,\mathrm{eV}$.

Cross Sections The capture cross section of the resonant isotope contains a single resonance, either a square resonance or a single-level Breit-Wigner resonance, with parameters described subsequently. The isotope has a potential scattering cross section of $11.4\,\mathrm{b}$ and no other reaction channels. The resonant material also contains non-resonant isotopes characterized by a background cross section of $8\,\mathrm{b}$. The number density of the resonant isotope is $0.022\,{}^{a}/_{\mathrm{b\cdot cm}}$. These values are consistent with U-238 in a light water reactor fuel pin.

The moderator is purely scattering and has macroscopic cross section $1.23\,\mathrm{cm}^{-1}$, representative of water in a pressurized water reactor.

Square Resonance For the case of a square resonance, the capture cross section takes some value in a small range in the center of the energy group and is zero elsewhere,

$$\sigma_\gamma(E) = \begin{cases} f & E_0 - \delta/2 \leq E \leq E_0 + \delta/2 \\ 0 & \text{otherwise} \end{cases}. \tag{1}$$

In this benchmark, f is varied, $E_0 = 1050\,\text{eV}$, and $\delta = 0.05\,\text{eV}$.

Single-Level Breit-Wigner Resonance For the case of a single-level Breit-Wigner resonance [2], the capture cross section is a single resonance. The resonance parameters are $\Gamma = 0.095\,\text{eV}$ and $\Gamma_n = 0.023\,\text{eV}$, which are taken from the resonance parameters from a real U-238 resonance at a similar energy. The center of the resonance is $E_0 = 1050\,\text{eV}$, and the temperature is $T = 300\,\text{K}$. The formula for the resonance is

$$\sigma_0(E) = \frac{\Gamma_n \Gamma_\gamma}{(\Gamma_n + \Gamma_\gamma)^2} \sqrt{\frac{E_0}{E}} r\psi(x,\xi), \tag{2}$$

where

$$r = \frac{2603911\,\text{b}\cdot\text{eV}}{E_0}\frac{A+1}{A} \tag{3}$$

$$x = \frac{2(E-E_0)}{\Gamma_n + \Gamma_\gamma} \tag{4}$$

$$\xi = (\Gamma_n + \Gamma_\gamma)\sqrt{\frac{A}{4kTE_0}} \tag{5}$$

$$\psi(x,\xi) = \Re\left(\frac{\xi\sqrt{\pi}}{2} W\left(\frac{(x+i)\xi}{2}\right)\right), \tag{6}$$

and $A = 238$ is the atomic mass, k is the Boltzmann constant, and $W(\cdot)$ is the Faddeeva function.

The size of the resonance is varied in this benchmark. This is accomplished by multiplicatively scaling this resonance to obtain a maximum cross section value f,

$$\sigma(E) = \sigma_0(E)\frac{f}{\max\limits_E \sigma_0(E)}. \tag{7}$$

Scattering Approximation Scattering is approximated as in the narrow resonance model. That is, all scattering is assumed to come from potential scattering resulting from a $1/E$ spectrum and a constant cross section Σ_p. This gives a scattering source in both fuel and moderator of

$$Q(E) = \frac{\Sigma_p}{E} \tag{8}$$

2.3 Transport Calculation

The transport calculation is performed using a collision probability approach. Because this problem has only two regions, this is a very simple calculation. Consider the collision probability form of the neutron transport equation, with the collision probabilities notated as P, the fuel or resonant region indexed as F, the moderator region indexed as M, and volumes given as V,

$$\Sigma^F(E)\phi^F(E)V^F = \left(1 - P^{F\to M}(E)\right) Q^F(E)V^F + P^{M\to F}(E)Q^M(E)V^M. \tag{9}$$

Invoking the reciprocity relation

$$V^F\Sigma^F P^{F\to M} = V^M\Sigma^M P^{M\to F} \tag{10}$$

and inserting Eq. 8, the transport equation simplifies to

$$\Sigma^F(E)\phi^F(E) = \left(1 - P^{F\to M}(E)\right) \frac{\Sigma_p^F}{E} + P^{F\to M}(E)\frac{\Sigma^F(E)}{E}. \tag{11}$$

For the case of the 1-D isolated slab, the collision probabilities are analytic,

$$P^{F\to M} = \frac{1}{2\Sigma^F d}\left(1 - 2E_3(\Sigma^F d)\right), \tag{12}$$

where d is the width of the slab and E_3 is the third exponential integral. For the 2-D pin-cell configuration, the collision probabilities were computed using a 2-D method of characteristics code.

2.4 Reference Solution

Because of the scattering approximation, the flux at a given energy is decoupled from that of any other energy. Thus, a reference can be obtained by solving a series of one-speed transport equations and performing an integration over energy. For the case of the square resonance, this integral is analytic; for the single-level Breit-Wigner resonance, this requires a numerical approach. The one-speed transport equation is solved using a collision probability model, as described in subsection 2.3.

3 SELF-SHIELDING METHODS DESCRIPTIONS

Here, brief descriptions of the self-shielding methods considered in initial studies with this benchmark are presented. This is not meant to be a complete list of self-shielding methods nor are the descriptions intended to be complete derivations.

3.1 Equivalence in Dilution

The method of equivalence in dilution [1, 2] notes that the two-region collision probability equation of Eq. 11 can be put in a form of an homogeneous medium equation, with all of the spatial

transport information lumped into a source term. The equivalent homogeneous medium equation is

$$\left(\Sigma^F(E) + \Sigma_{eq}(E)\right)\phi^F(E) = \frac{\Sigma_p^F}{E} + \frac{\Sigma_{eq}(E)}{E}. \tag{13}$$

with the equivalence cross section given by

$$\Sigma_{eq}(E) = \frac{P^{F\to M}(E)\Sigma^F(E)}{(1 - P^{F\to M}(E))}. \tag{14}$$

Note that when Σ_{eq} is constant in energy, this form is particularly convenient. It is equivalent to an infinite medium with an additional background moderator with cross section Σ_{eq}. Thus, dilution tables can be generated as cross sections from homogeneous medium calculations as a function of the background level, and they can be used directly in equivalent heterogeneous geometries.

3.1.1 Dancoff Factor

In approximations for the collision probabilities for two-region problems, it is often assumed that the resonant material is present in an isolated lump. That is, a neutron that escapes from the resonant material is guaranteed to have its next collision in the surrounding moderator. However, in realistic geometries, there are typically other lumps of resonant materials nearby. For instance, in a light water reactor, a neutron that escapes from a fuel pin has a significant chance of having its next interaction in a neighboring fuel pin rather than the water.

The Dancoff factor C is used to account for this effect [2]. It is defined as the probability that a neutron escaping a resonant region travels through the moderator and has its next collision with another lump of resonant material. In this study, the black Dancoff factor is used. That is, in the calculation of C, it is assumed that the cross section of the resonant material is infinite. The Dancoff factor is 0 when a fuel lump is isolated. The Dancoff factor approaches 1 as the lattice is tightened or the moderator density is reduced.

Here, the Dancoff factor was computed for the 2-D reflected pin-cell configurations by comparing the fuel to moderator collision probabilities for two cases, one with an isolated pin (equivalent to an infinite moderator cross section) and one in the benchmark configuration. In both cases, the fuel cross section was taken to be infinite, and a uniform isotropic source was placed in the fuel material. The obtained Dancoff factors were 0.1452, 0.2485, and 0.6202 for the cases of $0.3\,\mathrm{cm}$, $0.4\,\mathrm{cm}$, and $0.6\,\mathrm{cm}$ radii, respectively.

3.1.2 Wigner's Rational Approximation

Wigner's rational approximation [2] approximates the fuel to moderator collision probability for an isolated fuel lump as

$$P^{F\to M} = \frac{\Sigma_e}{\Sigma^F(E) + \Sigma_e}, \tag{15}$$

where a geometric parameter known as the escape cross section is given as $\Sigma_e = 1/\bar{l}$ and $\bar{l}$ is the mean chord length of the fuel lump. This approximation was made to ensure the collision probability performed as expected at the high cross section and low cross section limits. With this form, the equivalence cross section takes a convenient form,

$$\Sigma_{eq} = \Sigma_e. \tag{16}$$

When the Dancoff effect is taken into account, the equivalence cross section becomes

$$\Sigma_{eq} = (1 - C)\Sigma_e. \tag{17}$$

Thus, cross sections for a fuel lump, taking spatial effects into account, can be obtained from a dilution table computed for a homogeneous medium, as the equivalence cross section is constant in energy.

3.1.3 Wigner-Bell

Although Wigner's rational approximation does behave as expected in the extreme limits of fuel cross sections, it was observed to underpredict the fuel to moderator collision probability in most situations. The simplest correction to this is to multiply Σ_e by a constant b. This is known as the Bell factor [2], and the appropriate values for various configurations have been tabulated. In this paper, a single value of $b = 1.15$ is used for all calculations. This is a representative value for typical light water reactor conditions. Note, though, that the Bell factor does not preserve the correct behavior at the high cross section limit, and so it should be varied and driven to 1 for high cross sections in realistic simulations.

With the Bell factor, the collision probability and equivalence cross section are given by

$$P^{F\to M} = \frac{b\Sigma_e}{\Sigma^F(E) + b\Sigma_e} \tag{18}$$

and

$$\Sigma_{eq} = b\Sigma_e. \tag{19}$$

When the Dancoff effect is taken into account, this becomes

$$\Sigma_{eq} = \frac{(1 - C)b\Sigma_e}{1 - C + Cb}. \tag{20}$$

3.1.4 Roman's/Carlvik's Two-Term Rational Approximation

Wigner's rational approximation is a one-term approximation to the fuel to moderator collision probability. Rational approximations with multiple terms are of course possible. In practice, it has been seen that moving to two terms greatly improves solutions. With properly chosen parameters, two-term expansions preserve the collision probability behavior at the high and low cross section limits, both in value and in derivative.

The two-term rational approximation is

$$P^{F\to M} = \beta\frac{\alpha_1\Sigma_e}{\Sigma^F(E)+\alpha_1\Sigma_e} + (1-\beta)\frac{\alpha_2\Sigma_e}{\Sigma^F(E)+\alpha_2\Sigma_e}. \tag{21}$$

For slab geometry, this expansion is known as the Roman two-term rational approximation. For the isolated slab case, the parameters are [7]

$$\alpha_1 = 1.4 \quad \alpha_2 = 5.4 \quad \beta = 1.1. \tag{22}$$

For cylindrical geometry, the expansion is known as the Carlvik two-term rational approximation, with parameters given as [7]

$$\begin{aligned} \alpha_1 &= \frac{5A+6-\sqrt{A^2+36A+36}}{2A+2} \\ \alpha_2 &= \frac{5A+6+\sqrt{A^2+36A+36}}{2A+2} \\ \beta &= \frac{\frac{4A+6}{A+1}-\alpha_1}{\alpha_2-\alpha_1}. \end{aligned} \tag{23}$$

where $A = {}^{(1-C)}/_{C}$. Note that in the isolated pin limit, these parameters go to

$$\alpha_1 = 2 \quad \alpha_2 = 3 \quad \beta = 2. \tag{24}$$

To use this in practice, one can use a homogeneous dilution table to obtain two cross section values, σ_1 with added dilution $\alpha_1\Sigma_e$ and σ_2 with added dilution $\alpha_2\Sigma_e$. The effective cross section is then

$$\sigma = \beta\sigma_1 + (1-\beta)\sigma_2. \tag{25}$$

3.2 Embedded Self-Shielding Method

The Embedded Self-Shielding Method (ESSM) [6] is an extension of the equivalence in dilution methods. It recognizes that although equivalence in dilution seeks an equivalence between a heterogeneous and homogeneous model, the parameters at which this equivalence holds are difficult to determine *a priori*. Instead, ESSM iterates between a heterogeneous model and a homogeneous model until equivalence is obtained.

The homogeneous model is a two-region model where the spatial dependence has been replaced by an equivalence cross section. Here, the narrow resonance model is used, and the homogeneous model is Eq. 13. ESSM assumes that Σ_{eq} is constant in energy and integrates the homogeneous equation over energy to obtain

$$(\Sigma_g^F + \Sigma_{eq,g})\phi_g^F = \Sigma_p^F\Delta u_g + \Sigma_{eq,g}\Delta u_g, \tag{26}$$

where g subscripts on the cross sections and flux refer to group averaged quantities as is typical in multigroup transport and Δu_g is the lethargy width of the group. Note that for this equation to hold, Σ_{eq} must be constant within an energy group but can vary from group to group.

The heterogeneous equation is the multigroup transport equation for the geometry of interest. Whatever resonance model is used in the homogeneous equation is used as the scatter source in the heterogeneous problem; in this presentation, the narrow resonance model is assumed. In general, this takes the form

$$\hat{\Omega} \cdot \nabla \psi_g(\vec{r}, \hat{\Omega}) + \Sigma_{t,g}(\vec{r}) \psi_g(\vec{r}, \hat{\Omega}) = \Sigma_p(\vec{r}) \Delta u_g. \tag{27}$$

For the case of this benchmark, this is simplified to the multigroup form of Eq. 11,

$$\Sigma_g^F \phi_g^F = \left(1 - P^{F \to M}\right) \Sigma_p^F \Delta u_g + P^{F \to M} \Sigma_g^F \Delta u_g, \tag{28}$$

where the collision probabilities are computed using the multigroup cross sections.

With these two models defined, the ESSM procedure is as follows:

1. Guess $\Sigma_{eq,g}$.
2. Compute cross sections from dilution table using $\Sigma_{eq,g}$.
3. Solve Eq. 27 with obtained cross sections.
4. Use obtained flux from heterogeneous equation, and solve Eq. 26 for $\Sigma_{eq,g}$.
5. Iterate, repeating steps 2–4 to convergence.

3.3 Subgroup Method

The subgroup method [3–5] recognizes that the flux used in self-shielding models (e.g., narrow resonance) depends only on the cross section and the asymptotic $1/E$ spectrum. Thus, in lethargy space, the flux can be written as only a function of the cross section. The presentation given here uses the narrow resonance model, but the method is applicable to other approximations. The narrow resonance flux as a function of only the cross section is

$$\phi_{NR}(\sigma^*(u)) = \frac{\sigma_b + \sigma_p^*}{\sigma_b + \sigma^*(u)}, \tag{29}$$

where $*$ is used to index the resonant isotope.

This allows a change of variables, or in some sense a shift to Lebesgue integration, resulting in an integral over cross section rather than energy in the condensation of multigroup cross sections. This is a convenient transformation, as the flux is a much smoother function of cross section than of energy.

A numerical quadrature is performed for this energy condensation,

$$\sigma_g = \frac{\sum_n w_n \sigma_n \phi(\sigma_n)}{\sum_n w_n \phi(\sigma_n)}. \tag{30}$$

The parameters for the quadrature $Q = \{w_n, \sigma_n\}$ are not easily defined, and one method for determining the quadrature is presented subsequently.

Once a quadrature is obtained, fixed source transport problems are solved for every subgroup level in each group. These problems use the scattering source from the resonance model, resulting in purely absorbing fixed source calculations. Thus, the subgroup fixed source problems are entirely decoupled from one another.

In general, the subgroup fixed source problems take the form

$$\hat{\Omega} \cdot \nabla \psi_n(\vec{r}, \hat{\Omega}) + N^*(\vec{r})(\sigma_n + \sigma_b)\psi_n(\vec{r}, \hat{\Omega}) = \Sigma_p(\vec{r}). \tag{31}$$

For the case of this benchmark, this is the equivalent of Eq. 11 in lethargy space,

$$N^*(\sigma_n + \sigma_b)\phi = \left(1 - P^{F \to M}\right) \Sigma_p^F + P^{F \to M} N^*(\sigma_n + \sigma_b), \tag{32}$$

where the collision probabilities are computed by using $\Sigma^F = N^*(\sigma_n + \sigma_b)$.

3.3.1 Quadrature Generation

Here, the fitting method for subgroup quadrature generation is presented, as this is the method used for the results in this study. Note that the details of the fitting method varies among researchers; one option is given here. Other quadrature generation methods are possible, including the direct subgroup method [8] and the moment method [9].

The fitting method takes a set of reference data and minimizes the deviation to the approximate data generated by the subgroup quadrature. Consider a reference set of group averaged cross sections using the narrow resonance model with various background levels. Let this set be given by $\{\bar{\sigma}_k\}$, where each $\bar{\sigma}_k$ is a reference cross section with corresponding background cross section $\sigma_{b,k}$.

Now consider the approximate group average cross sections generated by the subgroup method with quadrature $Q = \{w_n, \sigma_n\}$. Let this set be given by $\{\tilde{\sigma}_k(Q)\}$, with

$$\tilde{\sigma}_k(Q) = \frac{\sum_n \frac{w_n \sigma_n}{\sigma_{b,k} + \sigma_n}}{\sum_n \frac{w_n}{\sigma_{b,k} + \sigma_n}}. \tag{33}$$

The quadrature Q is obtained by performing a least squares fitting procedure,

$$Q = \arg\min_{Q'} \sum_k \left(\frac{\bar{\sigma}_k - \tilde{\sigma}_k(Q')}{\bar{\sigma}_k} \right)^2. \tag{34}$$

This process is constrained such that the weights sum to unity and are nonnegative.

In this study, the cross section used in the fitting procedure was the capture cross section, as this allows the parameter of interest in the benchmark to be computed accurately. Note that σ_n in Eq. 32 refers to the total cross section, and so σ_p must be added to the cross section generated in this fitting procedure for use in the transport calculation. For all results given here, six subgroup levels were used.

4 RESULTS

Each self-shielding technique previously described was tested on the benchmark for various configurations. Results are presented in tabular form, showing the dependence on the height of the resonance. The reference solution is calculated using a calculation with ultrafine energy discretization as described in subsection 2.4. Performance of each method is described as the percent error of the obtained group averaged capture cross section compared to this reference. Positive errors represent obtained cross sections greater than the reference; negative errors represent obtained cross sections less than the reference.

First, results with a square resonance in the 1-D isolated slab geometry are presented. Table I gives results with a width of $0.3\,\mathrm{cm}$; Table II, with a width of $0.4\,\mathrm{cm}$; and Table III, with a width of $0.6\,\mathrm{cm}$. Note that subgroup results are not included, as the appropriate selection of a subgroup quadrature results in an exact solution for this simple case.

Next, results with a single-level Breit-Wigner (SLBW) resonance in the 1-D isolated slab geometry are given. Table IV gives results with a width of $0.3\,\mathrm{cm}$; Table V, with a width of $0.4\,\mathrm{cm}$; and Table VI, with a width of $0.6\,\mathrm{cm}$.

Finally, results with a SLBW resonance in the 2-D reflected pin-cell geometry are included. Table VII gives results with a pin radius of $0.3\,\mathrm{cm}$; Table VIII, with a pin radius of $0.4\,\mathrm{cm}$; and Table IX, with a pin radius of $0.6\,\mathrm{cm}$.

4.1 Equivalence in Dilution

Fig. 1 and Fig. 2 plot the error for the equivalence in dilution results as a function of the resonance peak for the 1-D slab cases with $0.4\,\mathrm{cm}$ width. The results are very familiar curves, behaving consistently with errors known for the rational approximations [7].

Wigner's rational approximation leads to very low error for small resonance peaks. For larger resonance peaks, this approximation does well for the square resonance, and slightly less so for the SLBW resonance. This is because although the peak of the resonance approaches the high cross section limit, the flanks of the resonance are in the intermediate cross section range where the approximation is less accurate. Furthermore, Wigner is seen to consistently underpredict the group averaged capture cross section, and is rather significant for intermediate resonance peaks.

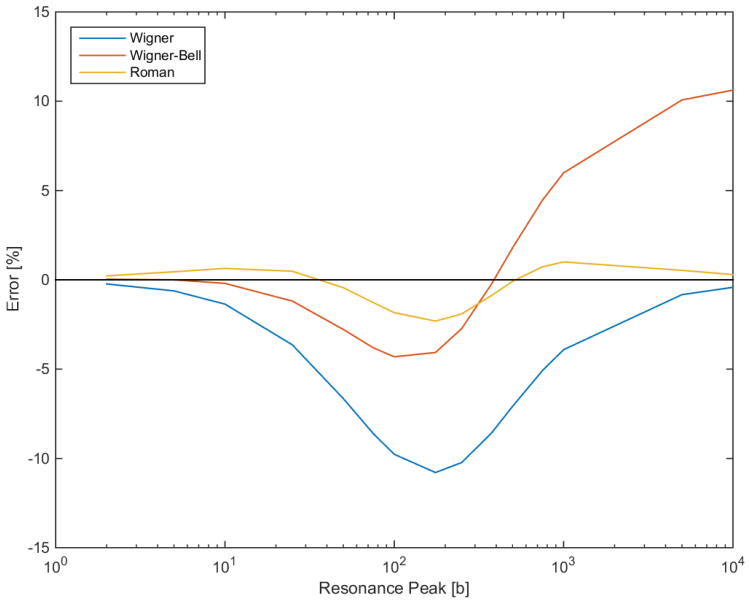

Figure 1. Error for equivalence in dilution techniques for 1-D isolated slab and a square resonance.

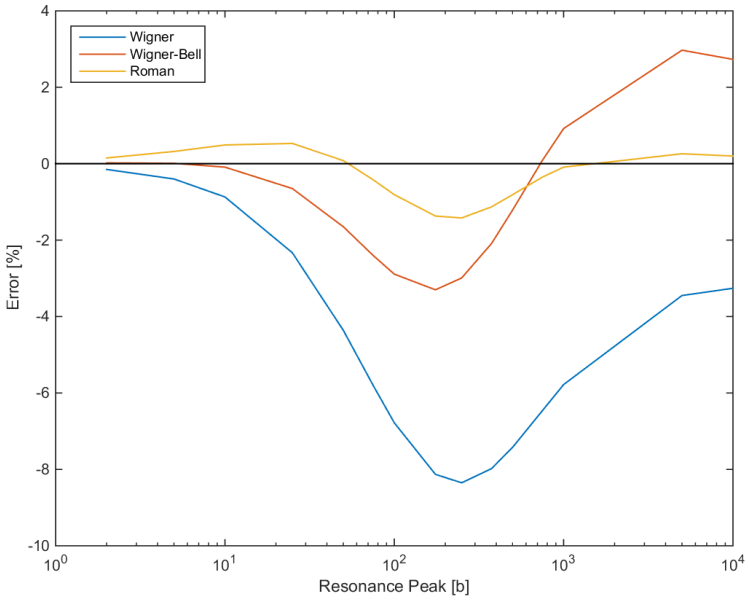

Figure 2. Error for equivalence in dilution techniques for 1-D isolated slab and a SLBW resonance.

The Wigner-Bell approximation shows the characteristic change of sign in the error at intermediate cross section values. It fares better than Wigner's rational approximation for low and intermediate resonance peaks, but does poorly for large resonance peaks. This is expected, as a single Bell factor was used for all calculations. At high opacities, it is known that the Bell factor should tend to unity, resulting in Wigner's rational approximation.

Roman's two-term rational approximation for the 1-D slab and Carlvik's two-term rational approximation for the 2-D pin-cell perform very well. For the square resonance case, errors are at or below 2%. For the SLBW resonance cases, nearly all errors fall below 1%. Clearly, a significant improvement is achieved by the inclusion of the second term in the rational approximation.

4.2 Embedded Self-Shielding Method

ESSM results are best for smaller resonance peaks, and the method appears to break down for larger resonances. This is somewhat counter-intuitive, as the iteration procedure is essentially searching for the appropriate Dancoff and Bell factor. Thus, one would expect ESSM to perform at least as well as the Wigner and Wigner-Bell approximations.

This can be explained primarily as ESSM being ill-conditioned. ESSM is forcing equivalence between heterogeneous and homogeneous models, using the flux as the connection. However, the flux varies over a very small range, and small changes in flux lead to very different implied shielding states. For physical intuition of this effect, consider widening the energy group, holding the single resonance constant. The group flux will approach unity for all shielding states, but the effective cross section will still be a strong function of the background. This means that a small error in flux leads to large errors in the obtained cross sections. For instance, in this benchmark, the heterogeneous problem suffers from small condensation errors, which is a well-known effect [10], and these errors are enough to impact the results.

Also, ESSM is essentially a direct subgroup method with a single level. Physically, the subgroup method is effective because it can differentiate the behavior of neutrons at resonance energies from those away from resonances. These cannot be separated with a single subgroup level, and the resulting effect is more pronounced for larger resonance peaks. So although it is mathematically possible to obtain an accurate quadrature with a single subgroup level, this is not realistic in practice. Thus, the ESSM procedure cannot be expected to accurately model self-shielding for large resonances.

4.3 Subgroup

The results for the subgroup method are very good, with nearly all errors falling below 1%. The variance in the errors can be attributed to the varying quality of the quadrature obtained in the fitting procedure for each configuration, as quadrature generation was found to be a difficult process, even for this simple problem. Adjustment of the subgroup parameters can lead to significant improvements in accuracy, but is not easily generalized. This suggests that subgroup can be an

effective self-shielding method, but it requires great care in the generation of the quadrature. For realistic simulations with many energy groups and isotopes, this is likely a very large effort.

It should be noted that using six subgroup levels in this study was an arbitrary choice, and this was more subgroup levels than necessary. Initial results with four subgroup levels provided similar accuracy. The issue of quadrature generation could be further explored using this benchmark and similar problems, comparing various quadrature generation methods and varying numbers of levels.

5 CONCLUSIONS

A simple benchmark has been presented here, which is the simplest problem in which both energy and spatial self-shielding effects are important. The benchmark was designed such that the assumptions made in the derivation of self-shielding models are fully valid. This allows self-shielding methods to be evaluated consistently and allows one to separate errors associated with the self-shielding method separately from any other effects.

This benchmark problem was solved using several techniques, including various equivalence in dilution methods, the Embedded Self-Shielding Method (ESSM), and the subgroup method. The best results were obtained using two-term rational expansions in the equivalence in dilutions methods and using the subgroup method. One-term rational expansion methods lead to much larger errors, as did ESSM.

Table I. Results for square resonance in 1-D isolated slab configuration with $0.3\,\mathrm{cm}$ width.

Peak [b]	Reference [b]	Error [%]			
		Wigner	Wigner-Bell	Roman	ESSM
2	0.0010	-0.13	0.09	0.26	-0.02
5	0.0024	-0.39	0.15	0.55	-0.13
10	0.0046	-0.92	0.09	0.85	-0.44
25	0.0102	-2.81	-0.60	0.97	-1.75
50	0.0174	-5.69	-2.09	0.28	-3.98
75	0.0227	-7.84	-3.29	-0.57	-5.69
100	0.0269	-9.35	-4.11	-1.28	-6.88
175	0.0348	-11.46	-4.89	-2.39	-8.39
250	0.0390	-11.69	-4.30	-2.49	-8.25
375	0.0425	-10.67	-2.36	-1.82	-6.82
500	0.0440	-9.28	-0.35	-0.99	-5.15
750	0.0454	-6.98	2.75	0.20	-2.49
1000	0.0459	-5.47	4.74	0.78	-0.77
5000	0.0472	-1.18	10.37	0.70	4.12
10000	0.0474	-0.60	11.15	0.40	4.79

Table II. Results for square resonance in 1-D isolated slab configuration with $0.4\,\mathrm{cm}$ width.

Peak [b]	Reference [b]	Error [%]			
		Wigner	Wigner-Bell	Roman	ESSM
2	0.0010	-0.23	0.03	0.22	-0.02
5	0.0024	-0.62	-0.00	0.45	-0.14
10	0.0045	-1.36	-0.20	0.64	-0.45
25	0.0098	-3.64	-1.19	0.48	-1.72
50	0.0162	-6.65	-2.78	-0.44	-3.63
75	0.0207	-8.60	-3.80	-1.27	-4.86
100	0.0240	-9.77	-4.31	-1.84	-5.53
175	0.0297	-10.79	-4.07	-2.31	-5.58
250	0.0325	-10.23	-2.73	-1.91	-4.43
375	0.0346	-8.58	-0.24	-0.88	-2.13
500	0.0356	-7.08	1.80	-0.08	-0.22
750	0.0364	-5.08	4.46	0.73	2.28
1000	0.0368	-3.91	5.99	1.00	3.72
5000	0.0378	-0.83	10.07	0.53	7.56
10000	0.0380	-0.42	10.62	0.29	8.08

Table III. Results for square resonance in 1-D isolated slab configuration with $0.6\,\mathrm{cm}$ width.

Peak [b]	Reference [b]	Error [%]			
		Wigner	Wigner-Bell	Roman	ESSM
2	0.0010	-0.38	-0.07	0.14	-0.02
5	0.0023	-0.97	-0.25	0.26	-0.13
10	0.0043	-1.97	-0.64	0.27	-0.42
25	0.0091	-4.57	-1.88	-0.24	-1.43
50	0.0144	-7.31	-3.24	-1.22	-2.55
75	0.0178	-8.63	-3.71	-1.78	-2.85
100	0.0200	-9.14	-3.61	-1.97	-2.64
175	0.0236	-8.64	-1.98	-1.50	-0.80
250	0.0252	-7.39	-0.05	-0.71	1.26
375	0.0263	-5.61	2.41	0.22	3.85
500	0.0269	-4.42	4.00	0.66	5.52
750	0.0274	-3.08	5.79	0.93	7.40
1000	0.0277	-2.35	6.76	0.93	8.41
5000	0.0284	-0.49	9.25	0.33	11.03
10000	0.0285	-0.25	9.58	0.18	11.38

Table IV. Results for SLBW resonance in 1-D isolated slab configuration with $0.3\,\mathrm{cm}$ width.

Peak [b]	Reference [b]	Error [%]				
		Wigner	Wigner-Bell	Roman	ESSM	Subgroup
2	0.0260	-0.08	0.06	0.17	-0.01	0.00
5	0.0637	-0.24	0.11	0.38	-0.07	-0.00
10	0.1238	-0.58	0.11	0.62	-0.24	-0.01
25	0.2861	-1.75	-0.24	0.85	-1.00	-0.11
50	0.5129	-3.62	-1.12	0.59	-2.36	-0.32
75	0.7007	-5.11	-1.91	0.14	-3.48	-0.49
100	0.8600	-6.25	-2.52	-0.29	-4.32	0.19
175	1.2244	-8.18	-3.44	-1.13	-5.66	-0.02
250	1.4831	-8.88	-3.55	-1.45	-5.99	-1.02
375	1.7886	-8.97	-3.04	-1.44	-5.67	0.54
500	2.0087	-8.61	-2.30	-1.19	-5.04	0.05
750	2.3256	-7.71	-0.96	-0.70	-3.79	0.93
1000	2.5612	-6.96	0.01	-0.36	-2.82	-0.60
5000	4.4141	-3.95	3.00	0.31	0.80	0.09
10000	5.8114	-3.57	2.96	0.28	1.30	-0.00

Table V. Results for SLBW resonance in 1-D isolated slab configuration with $0.4\,\mathrm{cm}$ width.

Peak [b]	Reference [b]	Error [%]				
		Wigner	Wigner-Bell	Roman	ESSM	Subgroup
2	0.0259	-0.15	0.02	0.15	-0.01	-0.00
5	0.0633	-0.40	0.01	0.32	-0.07	-0.01
10	0.1222	-0.87	-0.09	0.49	-0.25	-0.04
25	0.2782	-2.33	-0.65	0.53	-0.99	-0.19
50	0.4886	-4.36	-1.65	0.08	-2.18	-0.40
75	0.6569	-5.80	-2.40	-0.42	-3.04	-0.53
100	0.7958	-6.78	-2.89	-0.81	-3.60	0.17
175	1.1017	-8.13	-3.30	-1.37	-4.12	-0.03
250	1.3115	-8.35	-2.99	-1.42	-3.85	-0.67
375	1.5558	-7.98	-2.09	-1.13	-2.97	0.49
500	1.7328	-7.42	-1.21	-0.81	-2.08	-0.20
750	1.9929	-6.46	0.09	-0.35	-0.75	1.22
1000	2.1913	-5.78	0.92	-0.09	0.13	-0.54
5000	3.8342	-3.45	2.97	0.26	2.73	0.06
10000	5.1046	-3.26	2.73	0.20	2.83	-0.14

Table VI. Results for SLBW resonance in 1-D isolated slab configuration with $0.6\,\mathrm{cm}$ width.

Peak [b]	Reference [b]	Error [%]				
		Wigner	Wigner-Bell	Roman	ESSM	Subgroup
2	0.0258	-0.25	-0.05	0.10	-0.01	-0.01
5	0.0626	-0.64	-0.15	0.19	-0.07	-0.04
10	0.1196	-1.29	-0.39	0.24	-0.23	-0.09
25	0.2656	-3.02	-1.17	0.02	-0.84	-0.30
50	0.4519	-5.01	-2.14	-0.56	-1.60	-0.47
75	0.5932	-6.14	-2.64	-0.97	-1.95	-0.47
100	0.7054	-6.76	-2.82	-1.20	-2.01	0.08
175	0.9419	-7.19	-2.45	-1.26	-1.42	-0.01
250	1.0996	-6.90	-1.71	-1.01	-0.54	0.02
375	1.2842	-6.19	-0.60	-0.59	0.72	0.33
500	1.4210	-5.60	0.22	-0.30	1.63	-0.36
750	1.6285	-4.79	1.23	-0.01	2.76	1.01
1000	1.7911	-4.28	1.80	0.11	3.39	-0.21
5000	3.2125	-2.82	2.76	0.18	4.57	-0.01
10000	4.3359	-2.82	2.37	0.10	4.26	-0.18

Table VII. Results for SLBW resonance in 2-D reflected pin-cell configuration with $0.3\,\mathrm{cm}$ radius.

Peak [b]	Reference [b]	Error [%]				
		Wigner	Wigner-Bell	Carlvik	ESSM	Subgroup
2	0.0260	-0.40	-0.26	-0.05	0.00	0.00
5	0.0639	-0.97	-0.64	-0.13	0.01	-0.00
10	0.1243	-1.83	-1.21	-0.25	0.02	-0.03
25	0.2873	-3.91	-2.58	-0.57	0.13	-0.18
50	0.5115	-6.22	-4.05	-0.93	0.49	-0.47
75	0.6924	-7.62	-4.88	-1.12	1.01	-0.64
100	0.8422	-8.48	-5.31	-1.18	1.62	0.21
175	1.1724	-9.43	-5.44	-0.98	3.58	-0.03
250	1.3991	-9.40	-4.93	-0.61	5.40	-0.67
375	1.6642	-8.83	-3.86	-0.05	7.83	0.56
500	1.8567	-8.19	-2.93	0.33	9.59	-0.22
750	2.1395	-7.18	-1.60	0.74	11.86	1.25
1000	2.3540	-6.48	-0.74	0.90	13.19	-0.47
5000	4.0977	-4.05	1.52	0.71	15.24	0.03
10000	5.4323	-3.85	1.36	0.54	14.07	-0.17

Table VIII. Results for SLBW resonance in 2-D reflected pin-cell configuration with $0.4\,\mathrm{cm}$ radius.

Peak [b]	Reference [b]	Error [%]				
		Wigner	Wigner-Bell	Carlvik	ESSM	Subgroup
2	0.0259	-0.44	-0.29	-0.07	0.00	-0.01
5	0.0631	-1.04	-0.70	-0.17	0.01	-0.03
10	0.1214	-1.93	-1.29	-0.32	0.04	-0.09
25	0.2724	-3.91	-2.59	-0.66	0.23	-0.32
50	0.4676	-5.82	-3.75	-0.95	0.76	-0.53
75	0.6163	-6.79	-4.24	-1.02	1.43	-0.52
100	0.7349	-7.27	-4.38	-0.98	2.14	0.08
175	0.9862	-7.50	-3.99	-0.61	4.13	-0.00
250	1.1552	-7.17	-3.31	-0.24	5.73	0.07
375	1.3539	-6.50	-2.32	0.18	7.60	0.36
500	1.5010	-5.94	-1.59	0.41	8.83	-0.31
750	1.7228	-5.16	-0.64	0.61	10.26	0.89
1000	1.8955	-4.66	-0.08	0.66	11.01	-0.17
5000	3.3810	-3.15	1.09	0.40	11.39	-0.00
10000	4.5462	-3.11	0.84	0.30	10.30	-0.12

Table IX. Results for SLBW resonance in 2-D reflected pin-cell configuration with $0.6\,\mathrm{cm}$ radius.

Peak [b]	Reference [b]	Error [%]				
		Wigner	Wigner-Bell	Carlvik	ESSM	Subgroup
2	0.0254	-0.21	-0.13	-0.01	0.00	-0.02
5	0.0603	-0.48	-0.29	-0.03	0.01	-0.09
10	0.1114	-0.84	-0.51	-0.04	0.03	-0.19
25	0.2293	-1.49	-0.86	-0.04	0.16	-0.35
50	0.3601	-1.92	-1.02	0.01	0.43	-0.09
75	0.4502	-2.03	-0.99	0.10	0.71	0.31
100	0.5186	-2.05	-0.90	0.16	0.94	-0.23
175	0.6606	-1.90	-0.61	0.31	1.48	0.01
250	0.7575	-1.73	-0.38	0.38	1.82	0.63
375	0.8760	-1.52	-0.11	0.43	2.15	-0.40
500	0.9679	-1.37	0.05	0.44	2.34	-0.09
750	1.1130	-1.18	0.24	0.43	2.53	-0.23
1000	1.2309	-1.07	0.34	0.41	2.61	0.01
5000	2.3270	-0.82	0.40	0.28	2.42	0.01
10000	3.2072	-0.83	0.31	0.27	2.29	0.06

6 ACKNOWLEDGMENTS

This research was performed under appointment of the first author to the Rickover Fellowship Program in Nuclear Engineering sponsored by Naval Reactors Division of the U.S. Department of Energy.

7 REFERENCES

[1] G. I. Bell and S. Glasstone, *Nuclear Reactor Theory*, Van Nostrand Reinhold Company (1970).

[2] P. Reuss, *Neutron Physics*, EDP Sciences, Les Ulis, France (2008).

[3] M. N. Nikolaev, "Comments on the probability table method," *Nuclear Science and Engineering*, **61**, pp. 286 (1976).

[4] L. B. Levitt, "The probability table method for treatiing unresolved neutron resonances in Monte Carlo calculations," *Nuclear Science and Engineering*, **49**, pp. 450 (1972).

[5] D. E. Cullen, "Application of the probability table method to multigroup," *Nuclear Science and Engineering*, **55**, pp. 387 (1974).

[6] M. L. Williams and K.-S. Kim, "The Embedded Self-Shielding Method," *PHYSOR 2012 – Advances in Reactor Physics Linking Research, Industry, and Education*, Knoxville, TN, April, 2012.

[7] R. J. J. Stammler and M. J. Abbate, *Methods of Steady State Reactor Physics in Nuclear Design*, Elsevier Science & Technology Books (1983).

[8] A. Yamamoto and D. Nott, *Lattice Physics Computation*, volume 1 of *Handbook of Nuclear Engineering*, pp. 913–1239, Springer, 2010.

[9] P. Ribon, "Probability tables and Gauss quadrature application to neutron cross sections in the unresolved energy range," *Proceedings of the Topical Meeting on Advances in Reactor Physics and Safety*, volume 1, pp. 280, Saratoga Springs, USA, 1986.

[10] A. Hébert, *Applied Reactor Physics*, Presses Internationales Polytechnique, Montreal, Canada (2009).